American Journal of Engineering and Applied Sciences

Original Research Paper

Equilibrium Studies and Optimization of Phosphate Adsorption from Synthetic Effluent Using Acid Modified Bio-Sorbent

[1]Babayemi, Akinpelu Kamoru and [2]Onukwuli, Okechukwu Dominic

[1]Department of Chemical Engineering, Chukwuemeka Odumegwu Ojukwu University, (formerly known as Anambra State University)Uli, Nigeria
[2]Department of Chemical Engineering, Nnamdi Azikiwe University, Awka, Nigeria

Article history
Received: 06-10-2017
Revised: 07-11-2017
Accepted: 23-11-2017

Corresponding Author:
Babayemi, Akinpelu Kamoru
Department of Chemical Engineering, Chukwuemeka Odumegwu Ojukwu University, (formerly known as Anambra State University)Uli, Nigeria
E-mail: akinbabs40@yahoo.com

Abstract: Adsorption potential of periwinkle shell (PRW), an agricultural waste, for the removal of phosphate from aqueous solution was investigated through equilibrium studies at various experimental conditions. PRW was carbonized and chemically activated with $1MH_2SO_4$ before it was subjected to characterization using Fourier Transform Infrared (FT-IR), Energy Dispersive X-ray (EDX) and Scanning Electron Microscopy (SEM). Adsorption data were analyzed using various kinetic and isotherm models. Statistical modeling through Central Composite Design (CCD) was also employed. The results showed that, FT-IR spectrum of the activated PRW shows many absorption peaks and a variety of functional groups such as –OH, -NH, C = O, C-H, C-N, CH_3 and CH_2 which explains its improved adsorption behavior on the colloidal particles. SEM shows the morphological changes with respect to the shape and sizes of the adsorption sites.EDX indicates the higher percentage composition of carbon (11.66%), Oxygen (63.18%) as important constituent elements for adsorption. Equilibrium data were well fitted to pseudo second order kinetic model and were best described by Langmuir Isotherm model at the temperature of 303K. Removal efficiency of 95.90% was obtained. A statistical model equation was developed for the adsorption process which reveals contact time as the most significant main effect for performance of the adsorbent.

Keywords: Adsorption, Phosphorus, Periwinkle, Equilibrium, Isotherm, Kinetics

Introduction

Phosphorous is an essential element for both animals and plants on the earth. It is needed for the growth of algal and other biological organisms (Xiong *et al*., 2011; Yeddou and Bensmaili, 2009) Phosphorus in natural waters is dissolved and particulate form. They exist as polyphosphates, orthophosphates and organic phosphates in aqueous solution (Czelej *et al*., 2016). The principal phosphorus compounds in wastewater are generally orthophosphates (Grubb *et al*., 2000; Jiang *et al*., 2008) municipal wastewater may contain from 4 to 15mg/l phosphorus as PO_4^{3-} (Akay *et al*., 1998)

However, inordinate quantity of phosphorus in water bodies results in extensive algae growth, exhaustion of dissolved oxygen, turbid, dirty, odorous and unhealthful surface waters and extinction of many aquatic animals (Bhargava and Sheldarkar, 1992). Against this background, it is vital that a solution be urgently found to stop further degradation of environmental quality and its associated inauspicious socio-economic effects on the large segment of the community. Several methods have been introduced to the removal of phosphorus from wastewater and the commonly used techniques include precipitation (Chen and Zhuang, 2003), biological treatment (Wang *et al*., 2009), use of synthetic organic and inorganic chemical and adsorption (Liu and Hesterberg, 2016; Babayemi and Onukwuli, 2016). Adsorption on activated carbons has been considered, among others, to be more dependable and effective due its simplicity and cost effectiveness (Xiaoli *et al*., 2015; Yin and Cui, 2006).

Table1: Previous adsorption studies on phosphorus

Adsorbent	Adsorption conditions	Maximum removal efficiency (%)	Reference
Activated carbon Produced from Tamarind Nutshell (TNSAC)	Effects of adsorbent dose and size on phosphate removal from wastewater	57	(Nafaa, 2002)
Slag and Fly ash	Phosphate removal efficiency of slag and fly ash at various operating conditions	96.9	(Safaa, 2013)
Iron hydroxide-egg shell Waste	The feasibility of using iron hydroxide egg shell waste for phosphate removal	73	(Yeddou and Bensmaili, 2009)
Activated carbon from dolomite mineral	Adsorption of phosphate from aqueous solution on dolomite minerals at different experimental conditions	>95	(Xiaoli *et al*., 2015)
Activated carbon from palm kernel shell	Adsorption capacity of palm kernel shell for the removal of phosphates from wastewater	93.54	(Bhargava and Sheldarkar, 1992)
Activated carbon from animal bone	Adsorption potential of animal bone for the removal of phosphates from wastewater	97	(Xiong *et al*., 2011)

Activated carbons are mostly produced from carbonaceous materials such as palm nut (Joseph and Philomena, 2011), sawdust (Zeng *et al*., 2004), prawn shell (Nafaa, 2002), animal bone, palm kernel shell and other raw materials. Their distinctive adsorption properties result from their high surface areas, adequate pore size distributions, broad range of surface functional groups and comparatively high mechanical strength. Activated carbons are largely used for the removal of unpleasant organic and inorganic impurities from domestic and industrial wastewater.

Producing and making use of activated carbons from periwinkle shell, being an agricultural waste, for such purpose will not only reduce the health risk and environmental concerns associated with the use of synthetic organic and inorganic chemicals but also provides an alternative means of waste reduction and reuse. Previous works on the adsorption of phosphorus from aqueous solution are presented in Table 1.

Materials and Methods

Preparation of Activated Carbon from Periwinkle

Periwinkle shells were obtained from a local market in Port Harcourt, Rivers State, Nigeria. The shells were soaked in hot water for about 1h to remove the decayed flesh that was responsible for the bad odour oozing from the shells. Thereafter, the shells were carefully washed and dried in an oven at 110°C for 24h.The dried material was weighed and carbonized in the muffle furnace at a temperature of 800°C for 2h. After cooling to room temperature, the carbonized material was manually crushed using mortar and pestle before sieving to a desired particle size. The quantity needed for equilibrium studies was weighed and activated. The material was activated through impregnation in 1MH_2SO_4 in a beaker for 12h during which the surface pores of the carbon is activated. The activated carbon was then washed continuously with distilled water until pH7, after which it was filtered and the residue dried in an oven at 110°C for 24 h and then packed in an air- tight sample bags for use.

Characterization of Activated Periwinkle Shell

Activated PRW was subjected to proximate analysis using standard method (Babayemi *et al*., 2015). Surface area was estimated using Sear's methods (Alzaydien, 2009). The presence of their functional groups was determined through FT-IR, constituent elements and surface morphologies were analyzed via EDX and SEM respectively.

Equilibrium Studies

An aqueous solution was prepared from phosphate rock obtained from Federal Superphosphate Fertilizer Company, Kaduna, Nigeria. The batch adsorption experiment was performed. The solution pH was measured with a digital pH meter. About 100 mg of PRW was transferred into a beaker containing 10ml of the solution and placed on the magnetic stirrer at 30°C. A rotational speed of 200rpm was maintained throughout and at time intervals of 30 min. At the end of agitation of 30 min., the solution was filtered and the filtrate was tested for residual concentration of phosphate in a UV-spectrophotometer. The same procedure was repeated for the rest of the dosages, pH and temperature intervals.

The percent removal of phosphate was determined using Equation 1:

$$E(\%) = \frac{C_0 - C_1}{C_0} x100 \quad (1)$$

where, C_0 and C_1 are the initial and residual phosphate concentrations respectively.

Kinetic Studies

Lagergren first-order, pseudo second order and intra-particle diffusion kinetic equations were employed to represent the adsorption of phosphorus on activated PRW.

Lagergren first-order equation (Greenlee *et al*., 2010; Li *et al*., 2006; Otero *et al*., 2003).

The equation takes the form:

$$\frac{d_{q_t}}{d_t} = K_1\left(q_e - q_t\right) \tag{2}$$

After the definite integration by applying the conditions $q_t = 0$ at $t = 0$ and $q_t = q_t$ at $t = t$, Equation 2 becomes:

$$\ln\left(q_e - q_t\right) = \ln q_e - K_1 t \tag{3}$$

where:

q_t: = Amount of adsorption at time t, $(min)(mg/g)^{-1}$

q_e = Amount of adsorption at equilibrium (mg/g)

K_1 = The rate constant of the equation $(1/min)$ and was determined experimentally from the slope and intercept of the plots

$\ln\left(q_e - q_t\right)$ = against t

Pseudo Second Order Equation (Zhang and Land, 2003)

The equation is expressed as:

$$\frac{d_{q_t}}{d_t} = K_2\left(q_e - q_t\right)^2 \tag{4}$$

After definite integration by applying the conditions $q_t = 0$ at $t = 0$ and $q_t = q_t$ at $t = t$, Equation 4 becomes:

$$1/q_t = \frac{1}{K_2 q_e^2} + t / q_e \tag{5}$$

where, k_2 the rate constant of pseudo second order equation and can be determined from the slope and intercepts of the plots of $1/q_t$ versus t.

Intra-Particle Diffusion Model

Role of diffusion in the adsorption process can be determined with intra-particle diffusion model (Babayemi, 2017; Venkata and Karthikeyan,1997):

$$q_t = K_d \mathrm{t}^{1/2} + \mathrm{C} \tag{6}$$

C = A constant and represents the boundary layer thickness

K_d: (mg/gmin$^{-1/2}$) = The intra-particle diffusion rate constant

According to Equation 6, the plot of q_t versus $t^{1/2}$ should be linear passing through the origin if the adsorption process obeyed the intra-particle diffusion model.

Adsorption Isotherms

Langmuir Isotherm

$$q_e = (K_L q_{max} C_e) / (1 + K_L C_e) \tag{7}$$

q_{max} is the maximum amount of adsorption corresponding to mono layer coverage $\left(\frac{mg}{g}\right)$ K_L is the Langmuir constant and is related to the measure of affinity of adsorbent for the adsorbed $(1/mg)$ (Nwabanne, 2010).

For correlation purpose, the equation is rearranged as follows:

$$\frac{1}{q_e} = \left[\frac{1}{K_L}.q_{max}\left(\frac{1}{C_e}\right) + \left(\frac{1}{q_{max}}\right)\right] \tag{8}$$

A linear plot of $\frac{1}{q_e}$ against $\frac{1}{C_e}$ has a slope and intercept corresponding to $\frac{1}{K_L}.q_{max}$ and $\frac{1}{q_{max}}$ respectively.

The favourability of the adsorption process to Langmuir isotherm can be confirmed through the separation factor:

$$R_L = 1/\left(1 + K_L C_0\right) \tag{9}$$

The value of R_L indicates whether the isotherm is irreversible ($R_L = 0$), favourable ($0<R_L<1$), linear ($R_L = 1$) or unfavourable ($R_L>1$), (Babayemi, 2014).

Freundlick Isotherm

$$q_{e=K_F C_e^{1/n}} \tag{10}$$

$\frac{1}{n}$ is a heterogeneity factor which is a measure of intensity of adsorbate on the adsorbent. For favourable adsorption ($0<n<1$), while $n>1$ represents unfavourable adsorption and $n = 1$indicates linear adsorption, if $n = 0$, adsorption the process is irreversible (Ghosh and Bhattacharyya, 2002). *KF* is the Freundlick constant.

The linear form of Equation 10 is:

$$\ln q_e = \ln K_F + \frac{1}{n}\ln C_e \tag{11}$$

Temkin Isotherm

$$q_e = \left[\left(\frac{RT}{b_T}\right)\right]\ln K_T + \left[(RT)/b_T \ln C_e\right] \quad (12)$$

b_T represents the adsorption potential of the adsorbent K_T is the Temkin constant (Eletta *et al*., 2016). A plot of q_e versus $\ln C_e$ gives a straight line graph from which the value of K_T and b_T can be obtained.

Results and Discussion

Characterization Results

Proximate Analysis

The proximate analysis of PRW samples is summarized and presented in Table 2.

SEM Results

The surface textures of PRW before and after adsorption are displayed in Plates 1a and b respectively. Some morphological changes were observed in the surface textures with respect to shapes and sizes, the surface also changed into a new shinning and large particles with whitish patches structures indicating the adsorption of phosphates on the surfaces of the activated PRW.

EDX Results

The characterization results of the EDX are presented in Table 3. It is evident from the table that, carbon and oxygen are the main constituents 11.66 and 63.18% respectively, indicating its suitability for adsorption.

FT-IR Results

FT-IR spectrum of the activated PRW shows many absorption peaks as presented in Fig. 1. Oxygen functional groups are said to be important characteristics of adsorbents because they determine their surface properties (Das *et al*., 2006). The broad stretching absorption peak at 3382.20 and 3975.42 cm^{-1} correspond to –NH and bounded –OH groups. The bands at 1602.9 and 1720 cm^{-3} represent C=O stretching vibration of carboxyl groups. Other significant band positions are noted at 1431.23 cm^{-3} indicative of scissoring and bending vibrations of CH_3 and CH_2 groups, 1144.79 cm^{-3} indicative of C-N stretching of C = O group, 884.39 cm^{-3} indicating bending vibration of C-H group and 596.99 cm^{-3} is assigned to alkane group.

Table 2: Proximate analysis results of activated PRW

Parameter	Quantity
Weight loss (%)	47.31
Ash content (%)	5.98
Volatile matter (%)	23.51
Moisture content (%)	2.50
Fixed carbon (%)	72.55
Bulk density (g/cm^3)	0.53
Surface area (m^2/g)	620.81
Iodine number (mg/g)	553.06

Table 3: Characterization results of PRW using EDX

Element Atomic (%)	App.conc.	Intensity	Wt.%	Atomic (%)
C	3.78	0.2842	7.12	11.66
O	57.74	0.6006	51.43	63.18
Al	19.48	0.8479	12.30	8.96
P	13.41	1.2137	5.91	3.75
S	16.53	0.8679	10.19	6.25
Ca	22.35	0.9604	12.45	6.11
Sn	0.84	0.7501	0.60	0.10

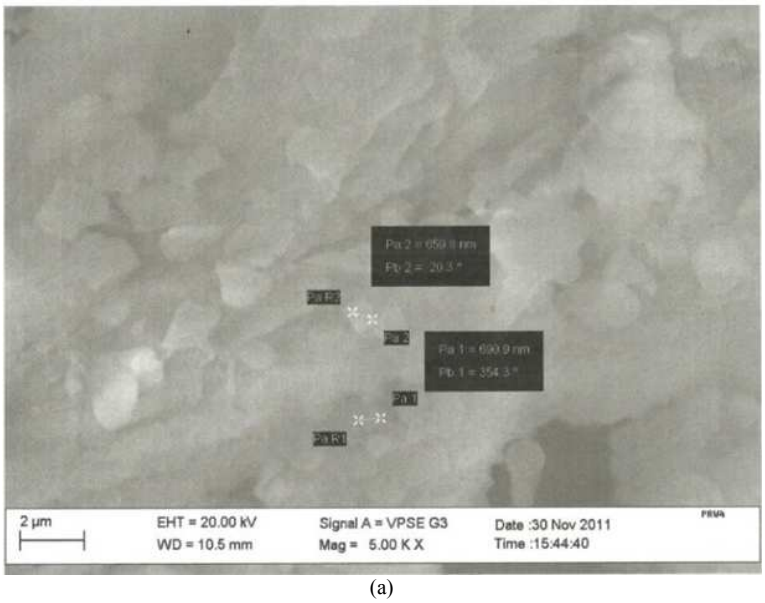

(a)

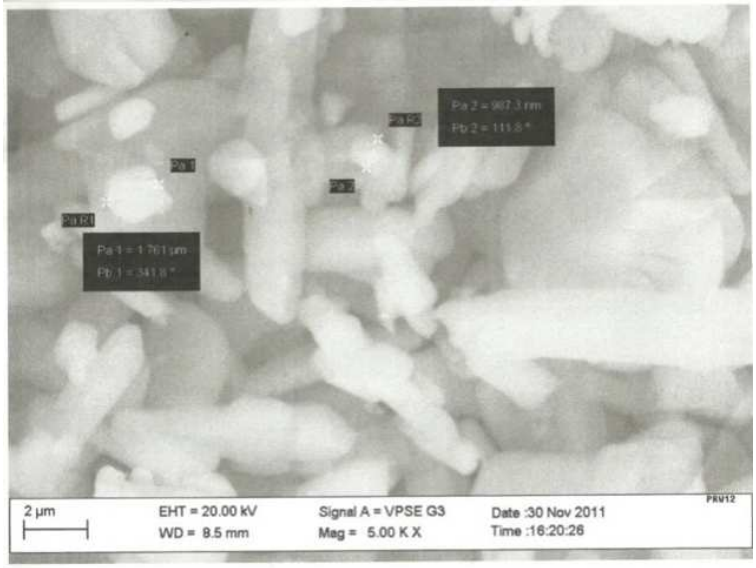

(b)

Plate 1: SEM images of PRW before and after adsorption

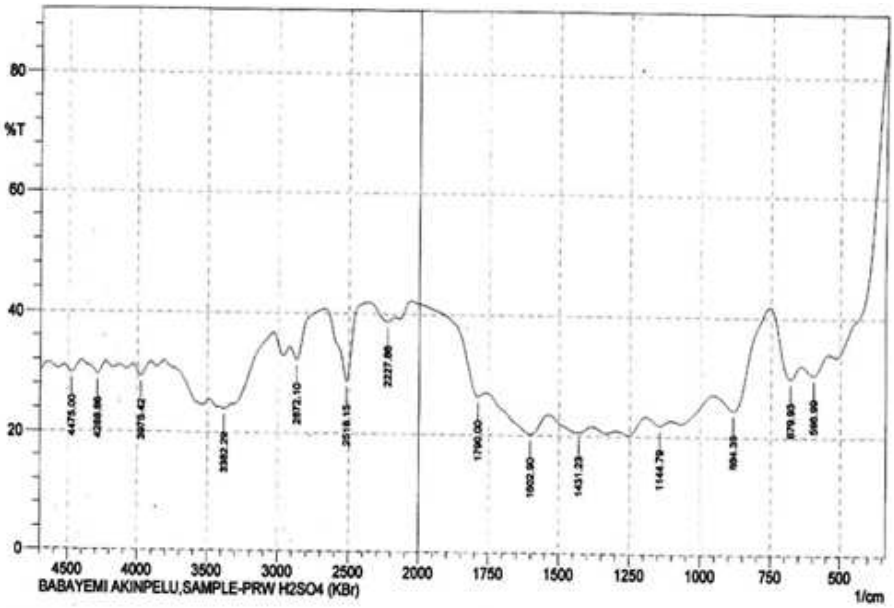

	Peak	Intensity	Corr. Intensity	Base (H)	Base (L)	Area	Corr. Area
1	596.99	30.5197	2.4505	640.39	542.98	48.4369	1.6173
2	679.93	29.8786	5.5847	754.19	640.39	53.6244	3.9806
3	884.39	24.4529	7.9782	958.65	754.19	105.6974	8.9823
4	1144.79	21.8383	1.1356	1193.98	1105.25	57.5671	0.9469
5	1431.23	20.5513	1.5531	1537.32	1386.86	100.3379	2.8478
6	1602.9	20.2199	4.33	1761.07	1537.32	143.3845	9.5282
7	1790	26.4008	2.1148	2061.01	1761.07	130.2266	-11.1111
8	2227.86	38.6963	1.5411	2359.02	2172.88	74.2333	1.5793
9	2518.15	28.7384	12.5783	2671.5	2359.02	135.6347	15.6977
10	2872.1	32.2382	3.3776	2921.29	2671.5	106.9623	0.306
11	3382.29	23.9323	0.491	3417.98	3329.25	54.7039	0.4573
12	3975.42	29.3727	2.0516	4033.29	3905.98	65.7477	1.7772
13	4288.86	29.5677	2.161	4405.56	4230.03	89.7577	2.2993
14	4475	29.8763	1.5479	4533.83	4405.56	65.8324	1.3954

Fig. 1: FT-IR spectrum of the activated PRW

Experimental Results

Effects of Contact Time on Phosphorus Adsorption

The removal efficiency of the activated PRW as a function of time is presented in Fig. 2. The rate of phosphate removal increases very fast within the first 60min. However, a gradual decrease in the removal efficiency with time was observed as the system approaches equilibrium between 180min and 240 min. Availability of the fresh active sites of PRW surfaces might be responsible for the fast rise in removal efficiency at the early stage of adsorption, but as the available sites are getting saturated by the adsorbates, there was less contact between the surface area of the adsorbent and the solute ion which in turn led to the observed decrease in the rate of phosphate removal.

Effect of Dosage on Phosphate Removal

Adsorbent dosage plays a vital role in the removal of phosphate as presented in Fig. 3.

As the adsorbent dosage was increased, more fresh active sites were made available for sorption, hence an increase in the removal efficiency. About 98.8% efficiency was obtained for a dosage of 50g/l at 300 min.

Effects of pH on Phosphate Adsorption

Normally, pH is viewed as one of the important parameters that control the adsorption at water-adsorbent interfaces (Das *et al*., 2006). The plot of percent removal of phosphate at various pH at different time intervals in minutes.(E30, E60, E120, E180, E240, E300) is presented in Fig. 4. It was observed that, as pH increased from pH2 to pH6 the amount of phosphate removed increased but further increase of pH brought about a steady decrease in removal. This may be as a result of the rising competition between OH^- groups and phosphate species $PO4^{3-}$ for the adsorption sites (Eletta *et al*., 2016).

Kinetic Studies

The kinetics parameters were evaluated and presented in Table 4. The adsorption data were well fitted to the pseudo second order kinetic model with the values of R^2 = 1.0000 at the chosen experimental temperatures. The deviation of straight lines from origin as presented in Fig. 5 implies that, the intra-particle transport is not the rate limiting steps and that pore diffusion is the only controlling step not film diffusion (Babayemi, 2014).

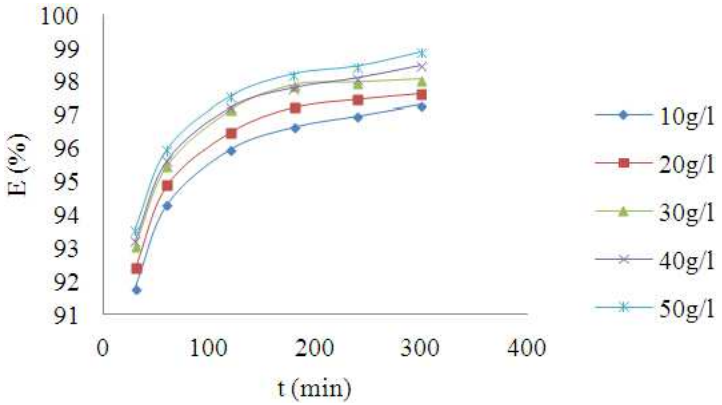

Fig. 2: Removal efficiency of PRW as a function of time

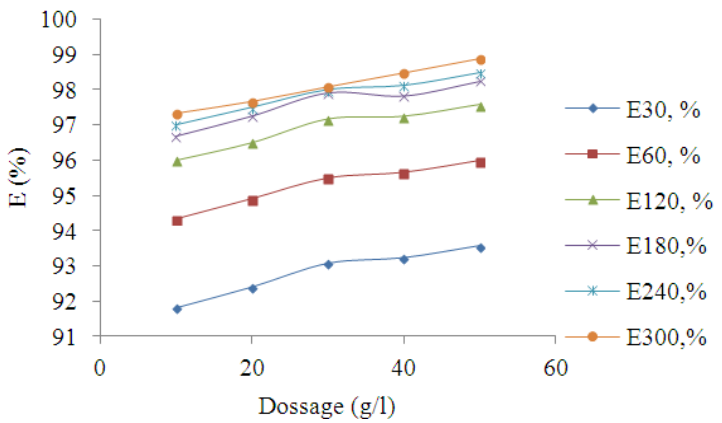

Fig. 3: Plot of removal efficiency of PRW at different adsorbent dosages

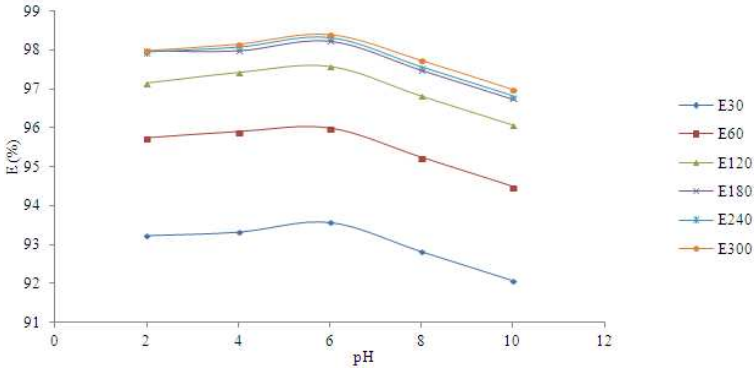

Fig. 4: Effects of pH on phosphate adsorption

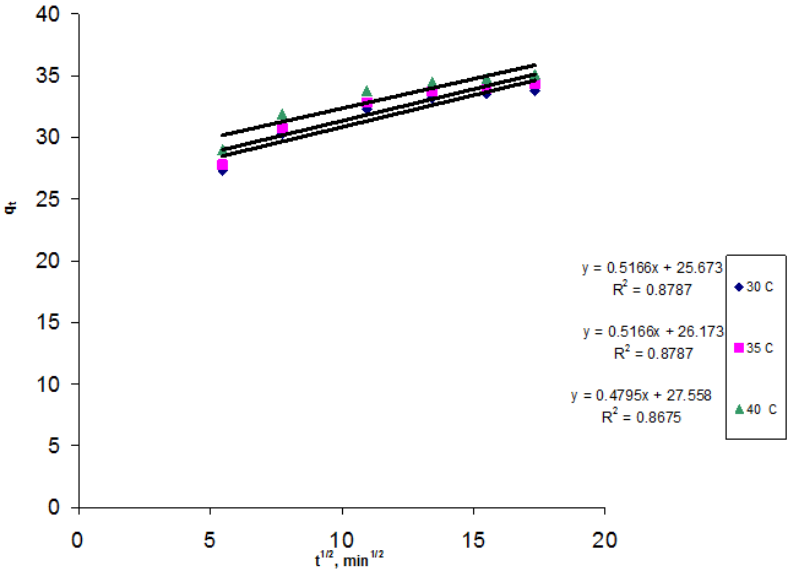

Fig. 5: Intra-particle diffusion plot for phosphate adsorption on PRW

Table 4: Evaluated kinetic parameters at different temperatures

Kinetic model equations	Parameters	303K	308K	313K
Lagergren first order				
$\frac{d_{q_t}}{d_t} = K_1(q_e - q_t)$	K_1(min^{-1})	0.0270	0.0135	0.0088
$\ln(q_e - q_t) = \ln q_e - K_1 t$	q_e(mg/g)	5.8835	2.9418	1.8748
	R^2	0.8144	0.8144	0.7929
Pseudo second order				
$\frac{d_{q_t}}{d_t} = K_2(q_e - q_t)^2$	K_2(g/mg.min^{-1})	0.0034	0.0034	0.0037
$1/q_t = \frac{1}{K_2 q_e^2} + t/q_e$	q_e(mg/g)	34.7222	35.2112	35.9712
	R^2	1.0000	1.0000	1.0000
Intra-particle diffusion				
$q_t = K_d t^{1/2} + C$	$K_d^{1/2}$(mg.gm^{-1}.mm$^{-1/2}$)	0.5166	0.5166	0.4795
	C	25.6730	26.1730	27.5580
	R^2	0.8787	0.8787	0.8675

Isotherm Models

The Langmuir, Freundlick and Temkin isotherm parameters were evaluated and presented in Table 5. The values of R_L indicate favourable adsorption of phosphorus on the activated PRW at all the chosen experimental conditions. The Freundlick constant 'n' being less than one (n<1) at all chosen temperatures also indicates favourable adsorption. The correlation coefficients R^2>0.9 confirms that the adsorption data fitted well to Langmuir and Freundlick isotherms but did not fit well toTemkin Isotherm R^2<0.9. The numerical fit results of non-linear regression analysis of the isotherm data are graphically presented in Fig. 6.

Statistical Modeling and Optimization

Statistical modeling Central Composite Design with a 2^3 full factorial design was employed.The adsorption process was modeled using the general equation:

$$Y = b_1x_1 + b_2x_2 + b_3x_3 + b_{12}x_1x_2 + b_{13}x_1x_3 + b_{23}x_2x_3 + b_{11}x_1^2 + b_{22}x_2^2 + b_{33}x_3^2$$

x_1,x_2 and x_3 are the coded values for pH, dosage and contact time respectively.

Table 5: Isotherm parameters for the adsorption of phosphorus on PRW

Isotherm model	Parameter	303K	308K	313K
Langmuir isotherm				
$q_e = (K_L q_{max} C_e)/(1 + K_L C_e)$	K_L	0.0221	0.0208	0.0178
	R_L	0.1082	0.1142	0.1309
$\frac{1}{q_e} = \left[\frac{1}{K_L}.q_{max}\left(\frac{1}{C_e}\right) + \left(\frac{1}{q_{max}}\right)\right]$	R^2	0.9466	0.9207	0.9151
Freundlick isotherm	n	0.3777	0.3395	0.3453
$q_{e=K_F C_e^{1/n}}$	K_F	0.0023	0.0006	0.0004
	R^2	0.9466	0.9271	0.8964
$\ln q_e = \ln K_F + \frac{1}{n}\ln C_e$				
Temkin isotherm	b_T	53.1000	55.8700	60.6700
	K_T	0.0467	0.0402	0.0549
$q_e = \left[\left(\frac{RT}{b_T}\right)\right]\ln K_T + \left[(RT)/b_T \ln C_e\right]$	R^2	0.7972	0.7423	0.8085

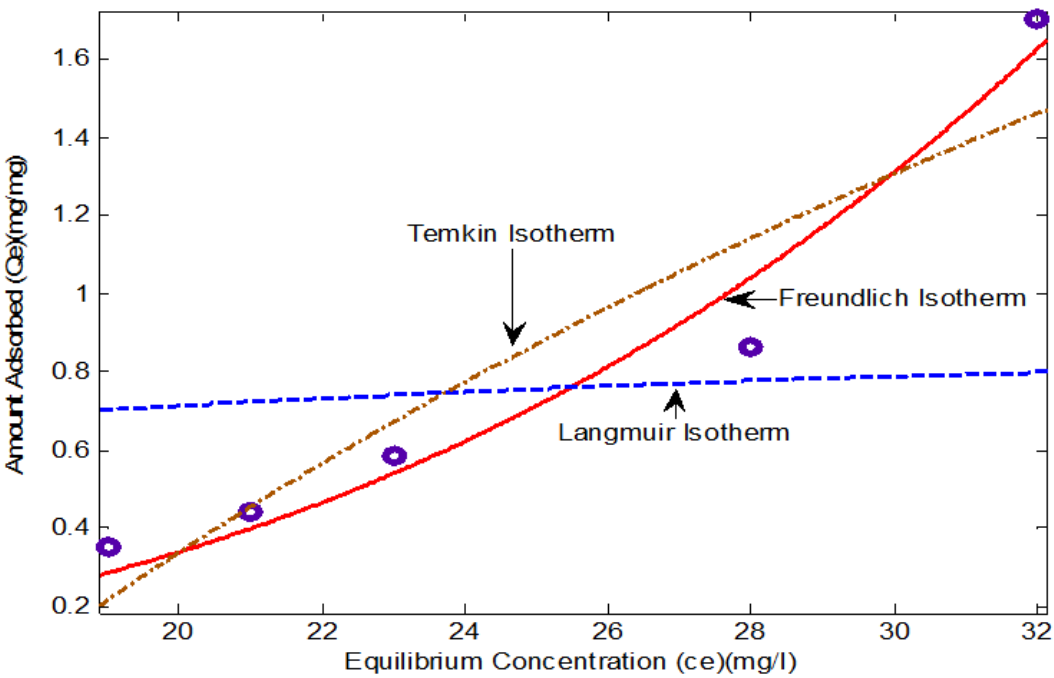

Fig. 6: Isotherm plot for fit to PRW

The obtained model fits for adsorption of phosphates on activated PRW after deleting the insignificant factors is given as:

$$Y = 94.2120 - 0.4247x_1 - 0.0465x_2 - 28.4349x_3 - 0.0002x_2x_3 + 0.1696x_1^2 + 0.000023x_2^2 + 3.4740x_3^2$$

The main attribute to effective performance of activated PRW is its contact time (P_{value} = 0.0000, Reg.coeff. = 0.4580). pH (P_{value} = 0.0777, Reg.coeff. = 0.1394) is also significant but not very effective. The interactions between adsorbent dosage and contact time x_2x_3 (P_{value} = 0.0000, Reg.coeff. = 0.5195) are also significant and very effective. Changes in either adsorbent dosage or contact time will have a major effect on the adsorption process. The surface response plot as presented in Fig. 7, 8 and 9. revealed a higher quadratic profile for contact time than for either dosage or pH. The model accuracy. The model accuracy is validated by the values of R^2(0.9902) and adjusted R^2(0.9787) and the closeness of the predicted values to the experimental values as presented in Fig. 10.

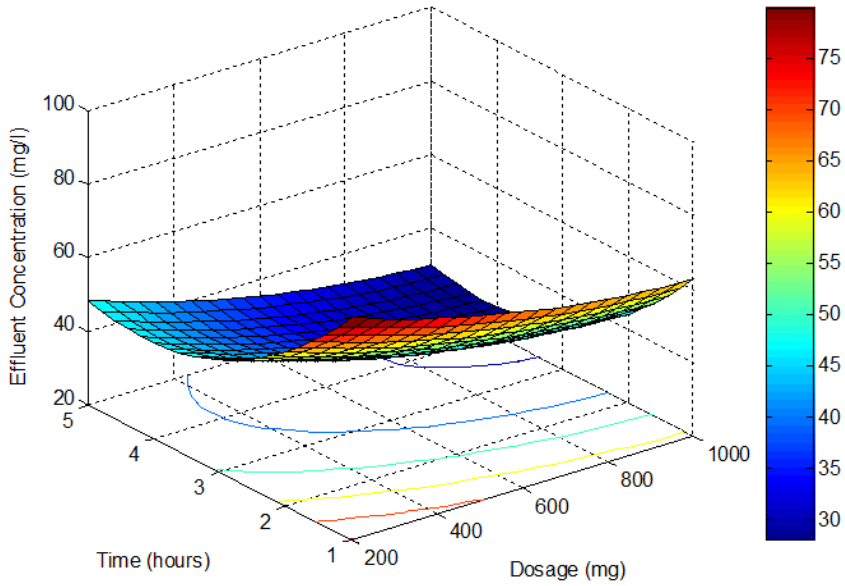

Fig. 7: 3-D plot for time-dosage

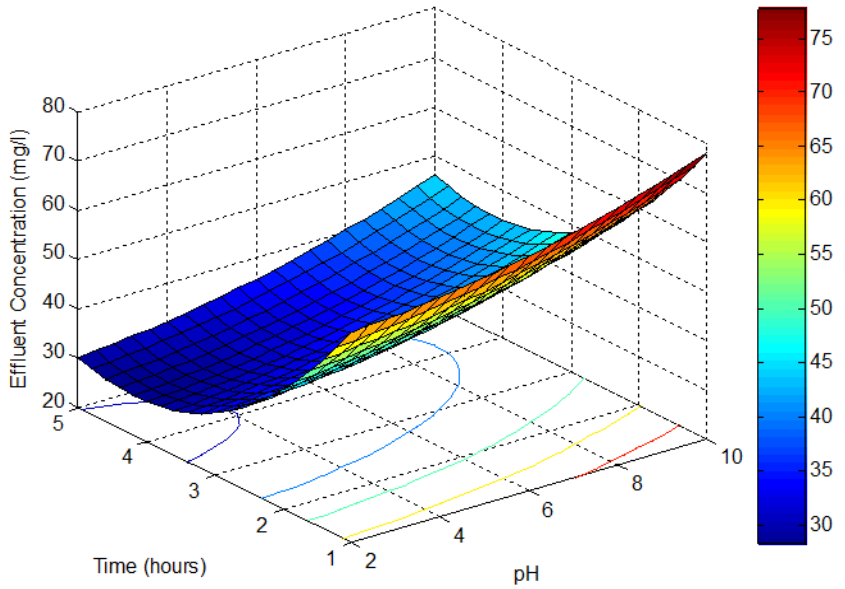

Fig. 8: 3-D plot for time-pH interactions

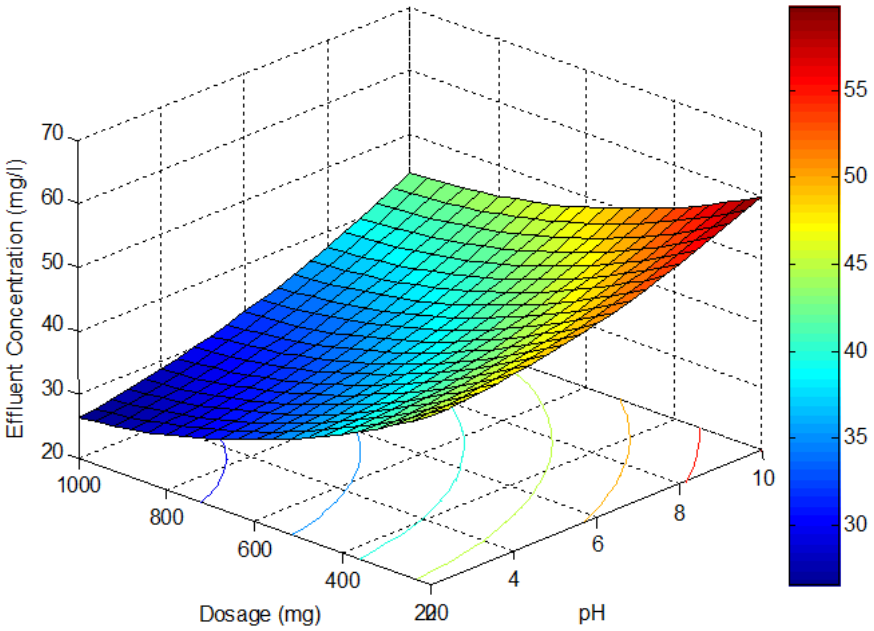

Fig. 9: 3-D plot for dosage- pH interactions

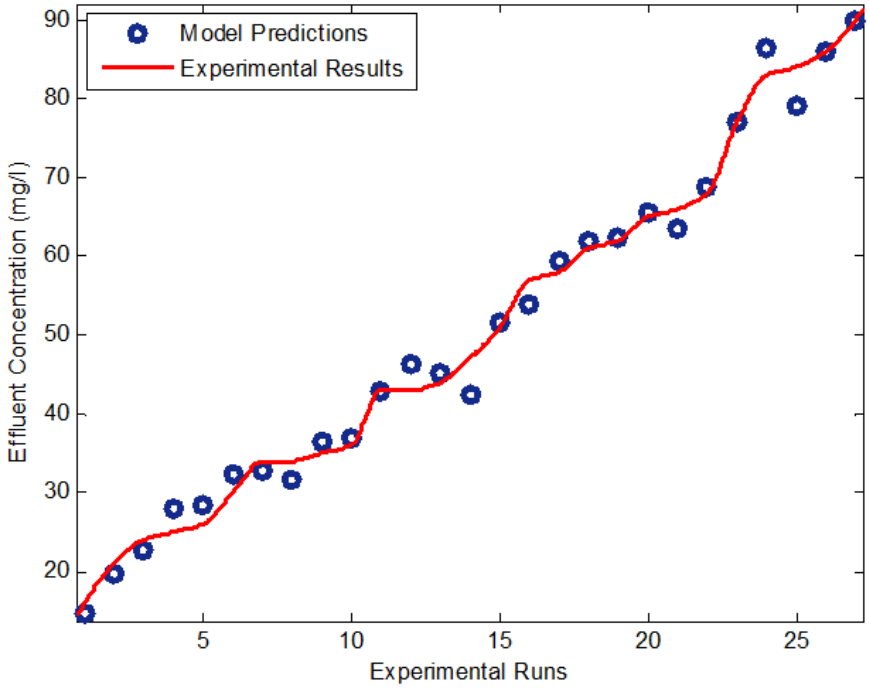

Fig. 10: Experimental versus predicted

Conclusion

This work has established acid modified periwinkle shell as a good potential, adsorbent for phosphate removal from aqueous solution being cost effective and non-toxic to the environment. The adsorptive performance of PRW was 95.90%. The adsorption data fitted well to pseudo second order kinetic model and were well described by Langmuir and Freundlick isotherms. A statistical model equation was developed for the adsorption process and the optimization response surface model established the minimum pH2, dosage (1000 mg) to be local while the contact time (4.1h) a global optimum for the process.

Acknowledgement

We express our gratitude to the staff of Federal Superphosphate Company, Kaduna for the supply of the phosphate rock used in this research.

Author's Contributions

Babayemi, Akinpelu Kamoru: Participated in all experiments, coordinated the data analysis and contributed to the writing of the manuscript.

Onukwuli, Okechukwu Dominic: Designed the research plan and organized the study.

Ethics

The authors declare there are no ethical issues that may arise after the publication of this manuscript.

References

Akay, G., B. Keskinler, A. Cakici and U. Danis, 1998. Phosphate removal from water by red mud using cross flow microfiltration. Water Res., 32: 717-726.

Alzaydien, A.S., 2009. Adsorption of methylene blue from aqueous solution unto a low cost natural Jordanian Tripoli. Am. J. Env. Sci., 6: 1047-1058. DOI: 10.3844/ajessp.2009.197.208

Babayemi, A.K. and O.D. Onukwuli, 2016. Adsorption isotherms, thermodynamics and statistical modeling of phosphate removal from aqueous by locally prepared bio-sorbent. J. Applied Chem., 9: 46-50. DOI: 10.9790/5736-0906024650

Babayemi, A.K., 2014. Removal of phosphorus from industrial and synthetic effluents using non conventional coag-flocculation and adsorption. Thesis of the unpublished dissertation in partial fulfilment of the requirement for the degree of PhDof Philosophy, Nnamdi Azikiwe University, Awka, Nigeria.

Babayemi, A.K., 2017. Performance evaluation of palm kernel shell adsorbents for the removal of phosphorus from wastewater. Adv. Chem. Eng. Sci., 7: 215-227. DOI: 10.4236/aces.2017.72016

Babayemi, A.K., O.D Onukwuli and A.O Okewale, 2015. Phosphorus removal from phosphate containing effluent using animal bone based activated carbon. Int. J. Eng. Sci. Res. Technol., 4: 421-426.

Bhargava, D.S. and S.B. Sheldarkar, 1992. Effects of adsorbent dose and size on phosphate removal from wastewaters. Environ. Pollution, 76: 51-60.

Chen, C.Y. and Y.Y. Zhuang, 2003. Adsorption equilibrium and kinetics of dyes on dried activated sludge. J. Safety Environ. 3: 46-50.

Czelej, K., K. Cwieka, J.C. Colmenares and K.J. Kurzydlowski, 2016. Insight on the interaction of methanol-selective oxidation intermediates with Au or/ and Pd containing Monometallic and Bimetallic core at Shell catalysts. Langmuir, 32: 7493-7502. DOI: 10.1021/acs.langmuir.6b01906

Das, J., B.S. Patra, N. baliarsingh and K.M. Parida, 2006. Adsorption of phosphate by layer double hydroxide in aqueous solutions. Applied Clay Sci., 32: 252-260. DOI: 10.1016/j.clay2006.02.005

Eletta, O.O.A., O.A. Ajayi, O.O. Ogunleye and I.C. Akpan, 2016. Adsorption of cyanide from aqueous solution using calcinated eggshells: Equilibrium and optimisation studies. J. Environ. Chem. Eng., 4: 1367- 1375. DOI: 10.1016/j.jece.2016.01.020

Ghosh, D. and K.G Bhattacharyya, 2002. Adsorption of methylene blue on kaolinite. Appli. Clay Sci., 2: 295-300. DOI: 10.1016/S0169-1317(01)00081-3

Greenlee, L.F., F. Testa, D.F. Lawler, B.D. Freeman and P. Moulin, 2010. The effects of antiscalant addition on calcium carbonate precipitation for a simplified synthetic brackish water reverse osmosis concentrate. Water Res., 44: 2957-2969. DOI: 10.1016/j.watres.2010.02.024

Grubb, D.C., M.S. Guimaraes and R. Valencia, 2000. Phosphate immobilization using acidic type fly ash. J. Hazard. Matter., 76: 217-236.

Jiang, Y., H. Pang and B. Liao, 2008. Removal of copper(II) ions from aqueous solution by modified bagasse. J. Hazardous Material, 64: 1-9. DOI: 10.1016/j.jhazmat.2008.07.107

Joseph, T.N. and P.I. Philomena, 2011. Copper (II) uptake by adsorption using Palmyra palm nut. Adv. Applied Sci. Res., 2: 166-175.

Li, Q., J.P. Zhai, W. Zhang, M. Wang and . Zhou, 2006. Kinetic studies of adsorption of Pb(II), Cr(III) and Cu(II) from aqueous solution by sawdust and modified peanut husk. J. Hazardous Materials, 141: 163-167. DOI: 10.1016/j.jhazmat.2006.06.109

Liu, Y.T. and D. Hesterberg, 2011. Phosphate bonding on non crystalline Al/Fe-hydroxide co precipitates. Environ. Sci. Technol., 45: 6283-6289. DOI: 10.1021/es201597j

Nafaa, A. and M. Lofti, 2002. Removal of cyanide from aqueous solution using impregnated activated carbon. Chem. Eng. Process, 41: 17-21.

Nwabanne, J.T., 2010. Adsorption and kinetic modeling of heavy metals uptake from wastewater effluents. Thesis of the unpublished dissertation in partial fulfilment of the requirement for the degree of PhD of Philosophy, Nnamdi Azikwe University, Awka, Nigeria.

Otero, M., F. Rozada, L.F. Calvo, A.J. Garcia and A. Mordn, 2003. Kinetic and equilibrium modeling of the methylene blue removal from solution by adsorbent materials produced from sewage sludges. Biochem. Eng. J., 15: 59-68. DOI: 10.1016/S1369-703x(02)001777-8

Safaa, M.R., 2013. Phosphate removal from aqueous solution using slag and fly ash. HBRC J., 9: 270-275. DOI: 10.1016/j.hbrcj.2013.08.005

Venkata, S. and J.M Karthikeyan, 1997. Removal of lignin and tannin colour from aqueous solution by adsorption onto activated charcoal. Environ. Pollut. 97: 163-197. DOI: 10.1016/S0269-7491(97)00025-0

Wang, F., S. Lu, Y. Wei and M. Ji, 2009. Characteristics of aerobic granule and nitrogen and phosphorus removal in a SBR. J. Hazardous Materials, 164: 1223-1227.

Xiaoli, Y., W. Xia, J. An, J. Yin and X. Zhou *et al*., 2015. Kinetic and thermodynamic studies on the phosphate adsorption removal by dolomite mineral. J. Chem., 2015: 1-8. DOI: 10.1155/2015/853105

Xiong, J.B., Y. Qin, E. Islam, M. Yue and W.F. Wang, 2011. Phosphate removal from solution using powdered fresh water mussel. Desalination, 276: 317-321. DOI: 10.1016/j.desal.2011.03.066

Yeddou, N.M. and A. Bensmaili, 2009. Kinetics and thermodynamic study of phosphate adsorption on iron hydroxide-eggshell waste. Chem. Eng. J., 147: 87-96. DOI: 10.1016/j.cej.2008.06.024

Yin, Y.B. and D.C. Cui, 2006. Sewage Treatment Technology of Constructed Wetland. 1st Edn., Chemical Industry Press, Beijing.

Zeng, L., X. Li and J. Liu, 2004. Adsorptive removal of phosphate from aqueous solutions using iron oxide tailings. Water Res., 38: 1318-1326. DOI: 10.1016/j.watres.2013.12.009

Zhang, X.J. and H.Y. Land, 2003. Synthesis and adsorption kinetics of the chelate compound of chitosan with ferrous ions. Chin. J. App. Chem., 20: 749-753.